Effect of surface induced nucleation of ferroelastic domains on polarization switching in constrained ferroelectrics

Rajeev Ahluwalia
Theoretical Division, Los Alamos National Laboratory, Los Alamos, New Mexico 87545

Wenwu Cao[a)]
Department of Physics and Materials Science, City University of Hong Kong, Kowloon, Hong Kong, China

(Received 23 July 2002; accepted 20 October 2002)

The role of the surface during polarization switching in constrained ferroelectrics is investigated using the time-dependent Ginzburg–Landau theory. The model incorporates the elastic and electrostrictive effects in the form of a long-range interaction that is obtained by eliminating the strain fields subject to the elastic compatibility constraint. A square-shaped finite sized constrained ferroelectric system with vanishing surface polarization is considered. Computer simulations of the hysteresis reveal that the corners of the constrained square act as nucleation sources for 90° domain structures. It is also found that no nucleation of the 90° domain structure takes place in a system with semi-infinite (corner free) geometry. For the corner free case, the polarization switches by 180° reorientations and a front of the reverse domains emerges from the surface, eventually sweeping over the entire system. Size dependence of the hysteresis loops is also studied. © *2003 American Institute of Physics.* [DOI: 10.1063/1.1529092]

I. INTRODUCTION

The spontaneous polarization in ferroelectrics can be switched by applying a strong electric field opposite to the polarization direction.[1] It is crucial to understand the details of this switching process due to many applications in memory devices and electromechanical systems. It is now a well established fact that the switching behavior is strongly influenced by nucleation, growth, and motion of domain walls. Due to the nucleation events, the experimentally measured coercive field is much smaller than the *intrinsic* value predicted by the simple one-dimensional Landau theory.[2] In a recent work,[3] we qualitatively showed that dipolar defects can act as nucleation centers for 90° domain structures. However, for a constrained system, such as a grain in a ferroelectric ceramic, the surface itself is a heterogeniety that can cause localized nucleation. Although, there have been some studies investigating the role of a surface on ferroelectric phase transitions,[4,5] the polarization switching in finite sized systems has not been well studied theoretically.

In this article, we present the results of a study on the influence of a surface during polarization switching using the time-dependent Ginzburg–Landau model described in Ref. 3. In particular, we are interested in understanding the role played by the surface in nucleating 90° ferroelastic domains during the switching process. Recent experiments on $BaTiO_3$ single crystals[6] have demonstrated the importance of 90° domains during polarization reversal. The theory incorporates elastic and electrostrictive effects in the form of an anisotropic long-range interaction obtained by eliminating strain fields, subject to the elastic compatibility requirement. Instead of using periodic boundary conditions (corresponding to a bulk system), we consider a finite sized constrained ferroelectric with the boundary condition of vanishing polarization at the surface. Physically, this corresponds to a system where the free charge at the surface is compensated. It is believed that this charge compensation occurs at the grain boundaries in ferroelectric ceramics. Due to the aforementioned boundary conditions, we can neglect the effects of the depolarization field. The nonlocal interaction is represented by the appropriate polarization gradients terms in the free-energy expansion.

The organization of this article is as follows. In Sec. II, we give details of the time-dependent Ginzburg–Landau model, starting from a free-energy functional for the polarization field. Section III gives details of our simulations of polarization switching for a finite square-shaped system. In Sec. IV, we describe simulations of switching behavior in a semi-infinite constrained system. We end the article by a summary and discussion of our results in Sec. V.

II. MODEL

The three-dimensional Ginzburg–Landau free energy for ferroelectric systems has been given in Ref. 7. In this work, we restrict ourselves to a two-dimensional system undergoing a square to rectangle transition, for which the total free energy is given by

$$F=\int d\mathbf{r}[f_l+f_g+f_{\mathrm{el}}+f_{es}+f_{\mathrm{ext}}], \tag{1}$$

where f_l is the local free-energy density given by

$$f_l=\frac{\alpha_1}{2}(P_x^2+P_y^2)+\frac{\alpha_{11}}{4}(P_x^4+P_y^4)+\frac{\alpha_{12}}{2}P_x^2P_y^2, \tag{2}$$

where P_x and P_y are the components of the polarization vector, α_1, α_{11}, and α_{12} are the free-energy parameters. The term f_g represents the gradient energy,

a)Electronic mail: apwwcao@cityu.edu.hk

 © 2003 American Institute of Physics

Downloaded 25 Jun 2003 to 128.118.103.146. Redistribution subject to AIP license or copyright, see http://ojps.aip.org/japo/japcr.jsp

$$f_g=\frac{g_1}{2}\left[\left(\frac{\partial P_x}{\partial x}\right)^2+\left(\frac{\partial P_y}{\partial y}\right)^2\right]+\frac{g_2}{2}\left[\left(\frac{\partial P_x}{\partial y}\right)^2+\left(\frac{\partial P_y}{\partial x}\right)^2\right]+\frac{g_3}{2}\left(\frac{\partial P_x}{\partial x}\right)\left(\frac{\partial P_y}{\partial y}\right), \tag{3}$$

where g_1, g_2, and g_3 are the gradient parameters. It has been shown that the gradient energy may be obtained as a local approximation to the nonlocal interactions.[1] The term f_{el} represents the usual elastic energy of the square system. We consider the bulk strain $\phi_1=(\eta_{xx}+\eta_{yy})/\sqrt{2}$, deviatoric strain $\phi_2=(\eta_{xx}-\eta_{yy})/\sqrt{2}$, and shear strain $\phi_3=\eta_{xy}=\eta_{yx}$. Here η_{ij} is the linear elastic strain tensor given as $\eta_{ij}=1/2(\partial u_i/\partial x_j+\partial u_j/\partial x_i)$, where u_i, $(i=x,y)$ represents the dispacement components. The elastic free energy can then be written as

$$f_{\text{el}}=\frac{a_1}{2}\phi_1^2+\frac{a_2}{2}\phi_2^2+\frac{a_3}{2}\phi_3^2, \tag{4}$$

where a_1, a_2, and a_3 are constants that can be expressed in terms of linear combinations of elastic constants of the system. The coupling energy f_{es} may be written as,

$$f_{es}=-q_1\phi_1(P_x^2+P_y^2)-q_2\phi_2(P_x^2-P_y^2)-q_3\phi_3P_xP_y. \tag{5}$$

Here, q_1, q_2, and q_3 are constants that are related to the electrostrictive constants of the system. The term f_{ext} is given by $f_{\text{ext}}=-\mathbf{E}_{\text{ext}}\cdot\mathbf{P}$. The amplitude of field $\mathbf{E}_{\text{ext}}$ is a tunable parameter in our simulations for studying polarization switching. We assume that the system reaches mechanical equilibrium very fast so that we may integrate out the elastic fields, subject to the elastic compatibility constraint.[8] In terms of the strain components ϕ_1, ϕ_2, and ϕ_3, the elastic compatibility relation is given as

$$\nabla^2\phi_1-\left(\frac{\partial^2}{\partial x^2}-\frac{\partial^2}{\partial y^2}\right)\phi_2-\sqrt{8}\,\frac{\partial^2}{\partial x\partial y}\phi_3=0. \tag{6}$$

To incorporate the elastic compatibility constraint, we consider an effective elastic part of the free energy $F_{\text{eff}}=F_{\text{el}}+F_{es}+F_{\text{cons}}$, with Lagrangian multiplier, λ, where

$$F_{\text{el}}=\int d\mathbf{k}\left\{\frac{a_1}{2}|\phi_1(\mathbf{k})|^2+\frac{a_2}{2}|\phi_2(\mathbf{k})|^2+\frac{a_3}{2}|\phi_3(\mathbf{k})|^2\right\}, \tag{7}$$

$$F_{es}=-\int d\mathbf{k}\{q_1\Gamma_1(\mathbf{k})\phi_1(-\mathbf{k})+q_2\Gamma_2(\mathbf{k})\phi_2(-\mathbf{k})+q_3\Gamma_3(\mathbf{k})\phi_3(-\mathbf{k})\}, \tag{8}$$

$$F_{\text{cons}}=\int d\mathbf{k}\{\lambda(\mathbf{k})(-k^2\phi_1(-\mathbf{k})+(k_x^2-k_y^2)\phi_2(-\mathbf{k})+\sqrt{8}k_xk_y\phi_3(-\mathbf{k}))\}. \tag{9}$$

Here, $k^2=k_x^2+k_y^2$ and $\Gamma_1(\mathbf{k})$, $\Gamma_2(\mathbf{k})$ and $\Gamma_3(\mathbf{k})$ are, respectively, the Fourier transforms of $P_x^2+P_y^2$, $P_x^2-P_y^2$, and P_xP_y. The condition of mechanical equilibrium and the compatibility relation demands $\delta F_{\text{eff}}/\delta\phi_i=0(i=1,2,3)$ and $\delta F_{\text{eff}}/\delta\lambda=0$.

$$\begin{aligned}a_1\phi_1(\mathbf{k})&=q_1\Gamma_1(\mathbf{k})+k^2\lambda(\mathbf{k}),\\ a_2\phi_2(\mathbf{k})&=q_2\Gamma_2(\mathbf{k})-(k_x^2-k_y^2)\lambda(\mathbf{k}),\\ a_3\phi_3(\mathbf{k})&=q_3\Gamma_3(\mathbf{k})+\sqrt{8}k_xk_y\lambda(\mathbf{k}),\end{aligned} \tag{10}$$

subject to the constraint

$$-k^2\phi_1(-\mathbf{k})+(k_x^2-k_y^2)\phi_2(-\mathbf{k})+\sqrt{8}k_xk_y\phi_3(-\mathbf{k})=0. \tag{11}$$

Using these equations, the multiplier $\lambda(\mathbf{k})$ is given as

$$\lambda(-k)=\frac{-k^2q_1\Gamma_1(-\mathbf{k})/a_1+(k_x^2-k_y^2)q_2\Gamma_2(-\mathbf{k})/a_2+\sqrt{8}k_xk_yq_3\Gamma_3(-\mathbf{k})/a_3}{k^4/a_1+(k_x^2-k_y^2)^2/a_2+8k_x^2k_y^2/a_3}. \tag{12}$$

At this stage, we make a simplification by assuming that the polarization electrostrictively couples only to the deviatoric strain. This assumption will not effect the qualitative behavior of the model in context of surface effects, which are the main focus of this article. We should also keep in mind that for the present case of a square to rectangle ferroelectric transition, the deviatoric strains are the dominant mode of deformation. The bulk and shear strains are usually localized at the domain walls for this case. Including the coupling with bulk and shear deformations may introduce intermediate metastable states with more complex patterns. Exclusion of these couplings makes the computation faster due to faster equilibriation. Finally, we should also mention that the neglect of this coupling in the free energy does not mean that bulk and shear strains will not be generated in this model at all. In fact, in this model, the strains are related to each other through the elastic compatibility relations which lead to the creation of bulk and shear strains, even under the approximation just described. In the limit of no coupling of polarization with shear and bulk strains, i.e. $q_1\to 0$ and $q_3\to 0$, using the equilibrium conditions and the Lagrange multiplier $\lambda(\mathbf{k})$, the free energy F_{eff} can be expressed in Fourier space as

$$F_{\text{eff}}=\frac{q_2^2}{2a_2}\int d\mathbf{k}H(\mathbf{k})|\Gamma_2(\mathbf{k})|^2, \tag{13}$$

where $H(\mathbf{k})=(h_1^2(\mathbf{k})/\alpha+h_2^2(\mathbf{k})-2h_2(\mathbf{k})+h_3^2(\mathbf{k})/\beta)$. The quantities $h_1(\mathbf{k})=k^2Q(\mathbf{k})$, $h_2(\mathbf{k})=\{1-(k_x^2-k_y^2)Q(\mathbf{k})\}$, and $h_3(\mathbf{k})=-\sqrt{8}k_xk_yQ(\mathbf{k})$, with $Q(\mathbf{k})$ defined as

$$Q(\mathbf{k})=\frac{(k_x^2-k_y^2)}{(k^4/\alpha+(k_x^2-k_y^2)^2+8k_x^2k_y^2/\beta)}. \tag{14}$$

Downloaded 25 Jun 2003 to 128.118.103.146. Redistribution subject to AIP license or copyright, see http://ojps.aip.org/japo/japcr.jsp

We have introduced dimensionless constants $\alpha = a_1/a_2$ and $\beta = a_3/a_2$.

The effective interaction derived herein is strongly direction dependent and is crucial to describe the domain-wall orientations. Similar anisotropic interactions have been considered in the context of martensitic transformations.[9,10]

As we wish to study heterogeneous nucleation, a dynamical formalism is needed to describe the nonequilibrium effects associated with domain switching. The time-dependent Ginzburg–Landau model for the polarization fields is used. We introduce rescaled time variables $t^* = (t|\alpha_1|L)(\alpha_1<0)$ (L is the kinetic coefficient), space variable $\mathbf{r}^* = \mathbf{r}/\theta$, the wave vector $\mathbf{k}^* = \mathbf{k}\theta$ ($\theta = \sqrt{g_1/a|\alpha_1|}$), where a is a dimensionless constant. The polarization field is transformed as $P_x = P_R u$ and $P_y = P_R v$, where $P_R = \sqrt{|\alpha_1|/\alpha_{11}}$ is the remnant polarization of the homogeneous state without elastic effects. With this set of parameters, the dimensionless time-dependent Ginzburg–Landau equations are given as

$$u_{,t^*} = u - u^3 - duv^2 + au_{,x^*x^*} + bu_{,y^*y^*} + cv_{,x^*y^*} + e_x - \gamma u \int d\mathbf{k}^* H(\mathbf{k}^*)\Gamma(\mathbf{k}^*)\exp(-i\mathbf{k}^*\cdot\mathbf{r}^*), \quad (15)$$

$$v_{,t^*} = v - v^3 - dvu^2 + av_{,y^*y^*} + bv_{,x^*x^*} + cu_{,x^*y^*} + e_y + \gamma v \int d\mathbf{k}^* H(\vec{\mathbf{k}}^*)\Gamma(\mathbf{k}^*)\exp(-i\mathbf{k}^*\cdot\mathbf{r}^*)$$

Here, $\mathbf{e} = \mathbf{E}_{\text{ext}}/(P_R|\alpha_1|)$ is the rescaled external electric field. The notation $u_{,t}$ represents the time derivative. The defined constants are: $b = (g_2/|\alpha_1|\theta^2)$, $c = (g_3/|\alpha_1|\theta^2)$, $d = (\alpha_{12}/\alpha_{11})$ and $\gamma = (q_2^2/\alpha_{11}a_2)$. The quantity $\Gamma(\mathbf{k}^*)$ is the Fourier transform of $(u^2 - v^2)$.

III. SIMULATION OF POLARIZATION SWITCHING FOR A CONSTRAINED SQUARE-SHAPED FERROELECTRIC

We now describe the details of our simulations on the switching behavior for a finite constrained ferroelectric. The long-range interaction is conveniently defined in Fourier space, which allows us to use the Fourier transform method. This reinforces the need to have periodic boundary conditions at the surfaces. To define a finite system using this scheme, we consider an 88×88 square region within a full simulation grid of size 128×128. The constraining is implemented by assuming that the polarization variables $u(\mathbf{r}^*)$ and $v(\mathbf{r}^*)$ vanish at the boundary and outside of the 88×88 region. This configuration represents an electromechanically clamped ferroelectric in which all displacements vanish at the surface. Equation (15) is discretized using the Euler scheme on the aforementioned grid. The space discretization step $\Delta x^* = \Delta y^* = 1$ and the time interval $\Delta t^* = 0.02$. The free-energy parameters chosen by us are $d = 2$ and $\gamma = 0.05$. The gradient coefficients are chosen as $a = b = c = 1$. Similarly, we choose the elastic parameter ratios as $\alpha = \beta = 1$. We first start from a random small amplitude initial conditions for the fields $u(\mathbf{r}^*)$ and $v(\mathbf{r}^*)$ and an external field $e_{x^*} = 10$. We solve Eq. (15) to obtain a single-domain configuration with the polarization oriented toward the $+x^*$ gradually decaying at the surface of the square system. Figure 1(a) shows this configuration corresponding to an electric field value $e_{x^*} = 10$. In Fig. 1(a), the arrows represent the local polarization vector (we have not shown all of the polarization vectors for the sake of legibility). Notice the gradual decay of the amplitude of the vectors in the surface region. This configuration is used as the initial state for the simulations of polarization switching. Equation (15) is now solved at each time step, starting from the initial configuration depicted in Fig. 1(a) with a time-dependent external field $e_{x^*} = (t^*)$. The time dependence is given as $e_{x^*} = e_0[1 - 2t^*/T]$, where $e_0 = 10$ is the initial electric field value and $T = 5000$ is the total number of simulated switching time steps. As the field decreases, the magnitude of the polarization vectors decreases uniformly everywhere in the simulated system at the beginning (keep in mind that the polarization is fixed to zero at the surface for all times). As the external electric field approaches zero, we observe that near two of the corners, the polarization vectors are distorted towards the [11] directions. Figure 1(b) shows the pattern corresponding to $e_{x^*} = 0.22$ where we can see the diagonal orientation of the polarization vectors near the corners. This indicates that shear strains are generated near the corners. The result is in agreement with recent simulations by Jacobs for a constrained ferroelastic system undergoing a square to rectangle transition where it was demonstrated that nondeviatoric strains are generated at the corners.[11,12] These diagonal shear strains at the corners are responsible for nucleation of 90° domain walls, as seen in Fig. 1(c) ($e_{x^*} = 0.199$) and Fig. 1(d) ($e_{x^*} = 0.0$). In Fig. 1(e) ($e_{x^*} = -0.199$), we can clearly see a well developed twinned structure with 90° domain walls. As we further decrease the field to $e_{x^*} = -0.38$, domains polarized along [01] direction grow at the expense of domains polarized along [10] directions, as can be seen by comparing Figs. 1(e) and 1(f). In Fig. 1(f) ($e_{x^*} = -0.38$), we can also observe that the dipoles in the vicinity of the corners and domain walls have started reorienting toward the $-x^*$ direction. Thereafter, the reversed domains grow at the expense of domains polarized along [01], and eventually all the dipoles are oriented along the $-x^*$ direction. This growth can be clearly seen from Figs. 1(g) ($e_{x^*} = -0.46$) and 1(h) ($e_{x^*} = -10$). Figure 1 illustrates the special role played by the corners during switching. The corners act as nucleation centers for 90° domain structures. Unlike the classically held belief of 180° reorientation of polarization, the switching takes place by sucessive 90° reorientations of the dipoles. Recently, evidence for such non-180° switching has been observed in rhombohedral single crystals of $Pb(Zn_{1/3}Nb_{2/3})O_3-PbTiO_3$.[13] The reverse cycle can be simulated by using the configuration in Fig. 1(h) as the initial condition and increasing the field as $e_{x^*} = e_0[1 - 2t^*/T]$, where $e_0 = -10$ and $T = 5000$ is the total number of switching time steps. Figure 2 shows the hysteresis loops obtained by plotting the average polarization $\langle u \rangle$ with the field e_{x^*}. The solid line in Fig. 2 corresponds to the situation depicted in Fig. 1 and the dashed line corresponds to this loop for the case without any surface (periodic boundary conditions). We can observe that for the case of the constrained square, the simulated hysteresis loop shows a long

Downloaded 25 Jun 2003 to 128.118.103.146. Redistribution subject to AIP license or copyright, see http://ojps.aip.org/japo/japcr.jsp

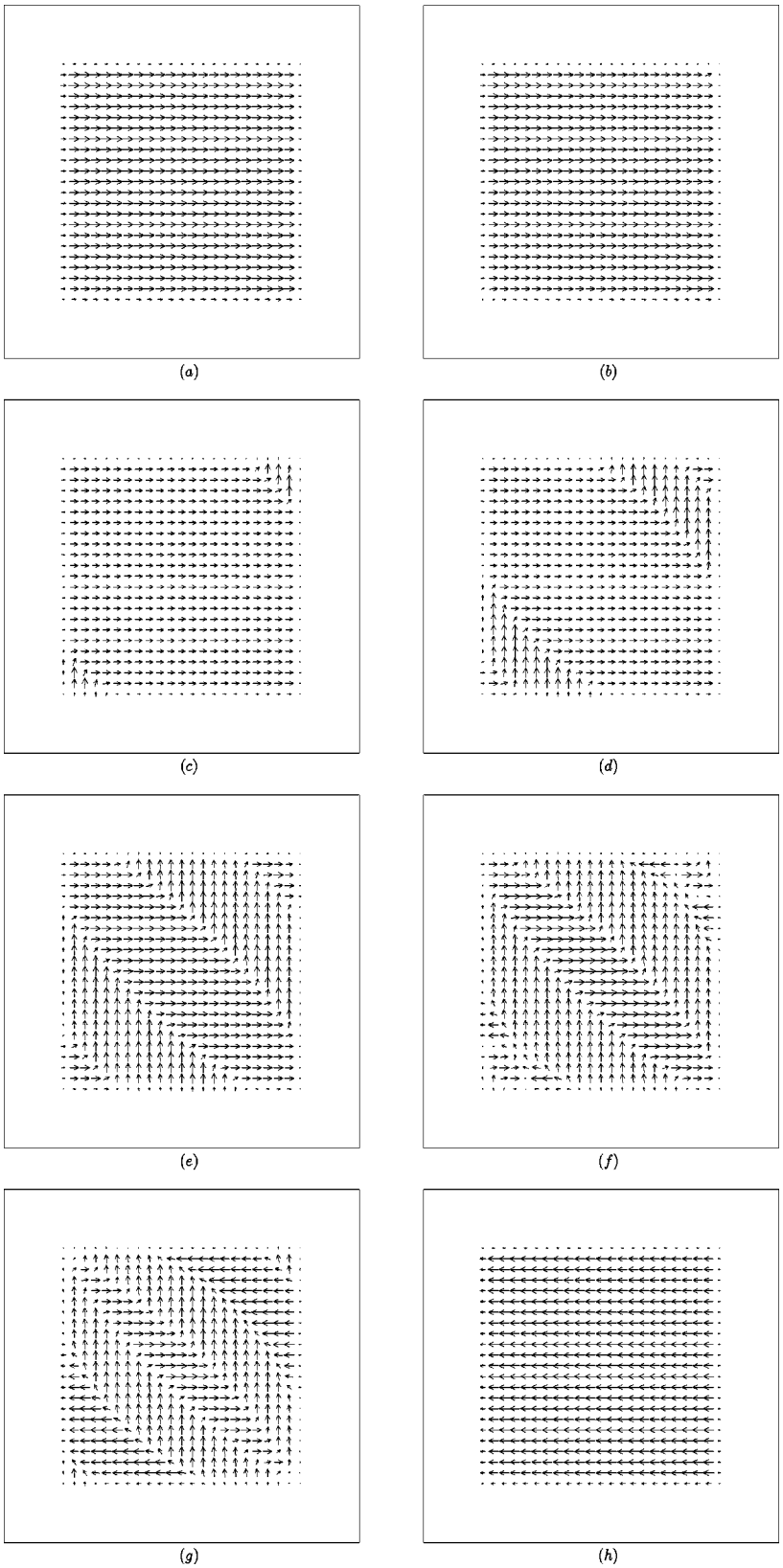

FIG. 1. Pattern evolution for the simulated switching in a constrained square. The snapshots correspond to (a) $e_{x*}=10$, (b) $e_{x*}=0.22$, (c) $e_{x*}=0.199$, (d) $e_{x*}=0$, (e) $e_{x*}=-0.199$, (f) $e_{x*}=-0.38$, (g) $e_{x*}=-0.46$, and (h) $e_{x*}=-10$.

''tail'' region where the forward and reverse cycle curves do not close up. This corresponds to the appearance and disappearance of the 90° domain pattern. In contrast, for the periodic boundary condition case, the hysteresis loop has no tail region as there are no nucleation events. We can also observe that the saturation polarization and remnant polarization fields are lower for the constrained system than that for the case with periodic boundary conditions. However, there is not much difference between the coercive fields of the two cases. We have simulated the hysteresis loops for different system sizes to study the size dependence of the switching phenomena. In Fig. 3, we show the simulated hysteresis

Downloaded 25 Jun 2003 to 128.118.103.146. Redistribution subject to AIP license or copyright, see http://ojps.aip.org/japo/japcr.jsp

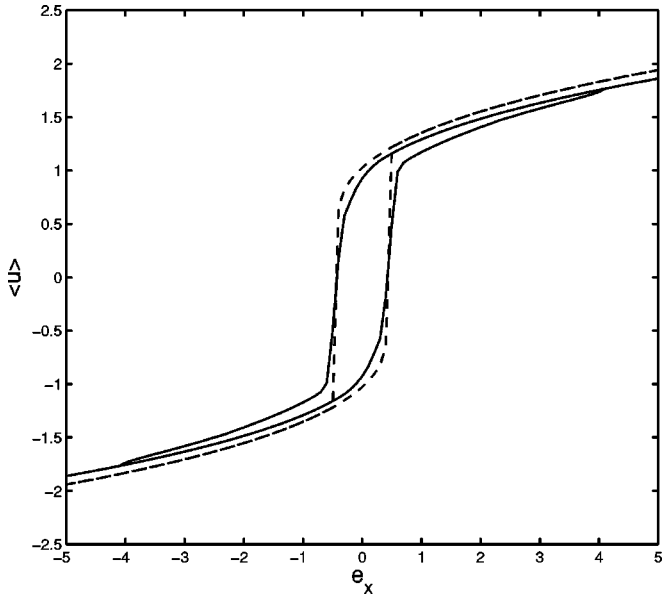

FIG. 2. Plots of $\langle u \rangle$ vs e_x showing the simulated hysteresis loops for the constrained square (solid line) and the periodic boundary condition case (dotted line).

loops for system sizes indicated at the top of each frame. A comparison of the loops for sizes $L=88$ and $L=68$ reveals that the coercive fields and the saturation polarization are almost the same for both systems. Also, the 90° domain structure is shorter lived for the smaller system since the tail region of the hysteresis loop for the $L=68$ system is smaller than that for the $L=88$ system. For smaller sizes, the domain pattern becomes increasingly short lived during the switching process, as can be concluded from the loop for $L=48$ where the tail has moved further inward. However, the saturation polarization and the coercive fields still do not show much variation. The tail almost disappears for the $L=20$ hysteresis loop and we see a small bump near the coercive field region. For this size, we can see a reduction in the coercive field as well as the saturation polarization due to the surface effects. Below this size, nucleation of 90° domains does not take place. The switching occurs by 180° reorientations that preferentially start at the surface. The hysteresis loops in this regime have a shape similar to the periodic boundary condition case. It is clear from Fig. 3 that upon further decreasing the size, the saturation polarization, remnant polarization and coercive field decrease rapidly. We can see that the hysteresis is very small for $L=6$ which is the smallest size simulated. For the present set of parameter values, we do not observe a ferroelectric to paraelectric transition for $L=6$. Such a transition was observed for a simulation with a much higher value of the gradient coefficients. The behavior observed in Fig. 3 can be understood in terms of size dependence of ferroelectric behavior. It is experimentally and theoretically established that the spontaneous polarization progressively decreases upon decreasing the size for a system in which the polarization is constrained to decay at the surface.[5,6,14,15] Thus, the remnant polarization, saturation polarization, and coercive field decrease upon decreasing the system size. The anisotropic nonlocal interaction responsible for the nucleation of 90° domain structures also decreases as the size is decreased. Thus for small sizes, the hysteresis loops are free of 90° nucleation. A similar transition from multidomain to single-domain states upon decreasing the size has been discussed in earlier works.[15,16] The main effect of size reduction comes from the surface layer under the vanishing polarization boundary condition. The transition temperature is effectively reduced and the energy barrier between the low-temperatures states is also lowered.

IV. SIMULATION OF POLARIZATION SWITCHING FOR A SEMI-INFINITE CONSTRAINED FERROELECTRIC

In this section, we describe switching behavior for a semi-infinite constrained ferroelectric system. Here we use periodic boundary conditions along the y direction and vanishing polarization conditions at the surface for the x direction. Figure 4 shows the dynamics of polarization switching for the semi-infinite case. Except for the boundary conditions, all other parameter values, including the time dependence of the switching field are the same as that for the case of the constrained square described in Sec. III. Figure 4(a) shows the fully polarized single-domain initial configuration for $e_{x*}=10$. In Fig. 4(b), we can see that a single domain persists even when the applied field is lowered to $e_x=-0.319$, although the polarization magnitude has decreased by a very small amount. As the field is further decreased to $e_{x*}\sim-0.36$, nucleation of the reversed polarization domains from the two surfaces takes place, as depicted in Fig. 4(c). The reversed domains grow larger and eventually into a single-domain crystal with reversed polarization. This reversed domain growth is clear from Fig. 4(d) ($e_{x*}=-0.399$) and Fig. 4(e) ($e_{x*}=-0.44$). Figure 4(f) shows the final state corresponding to $e_{x*}=-10$. Figure 4 illustrates the fact that for the corner free semi-infinite geometry, the reversal occurs only by 180° reorientations. The hysteresis loop corresponding to the situation shown in Fig. 4 can be computed. In Fig. 5, we plot the hysteresis loop for the case shown in Fig. 4 along with the loop for the surface free case with the periodic boundary conditions. Unlike the case shown in Fig. 2, the hysteresis loops for the surface free case and the semi-infinite case have the same shape. However, the saturation polarization, the remnant polarization, and the coercive field are slightly smaller for the semi-infinite case due to the suppressed transition at the surface. We have also simulated the size dependence for this case and found that the hysteresis loops become progressively narrower with decreasing size without any shape change. This is due to the fact that there are no 90° domains and the long-range elastic interaction does not play any role in this case.

V. SUMMARY AND DISCUSSION

We have simulated the switching behavior in constrained ferroelectrics with the boundary condition of vanishing polarization at the surface. A square-shaped system is considered along with a system with semi-infinite geometry. We find that the corners of the square-shaped system nucleate 90° domains and the switching is dominated by the motion

Downloaded 25 Jun 2003 to 128.118.103.146. Redistribution subject to AIP license or copyright, see http://ojps.aip.org/japo/japcr.jsp

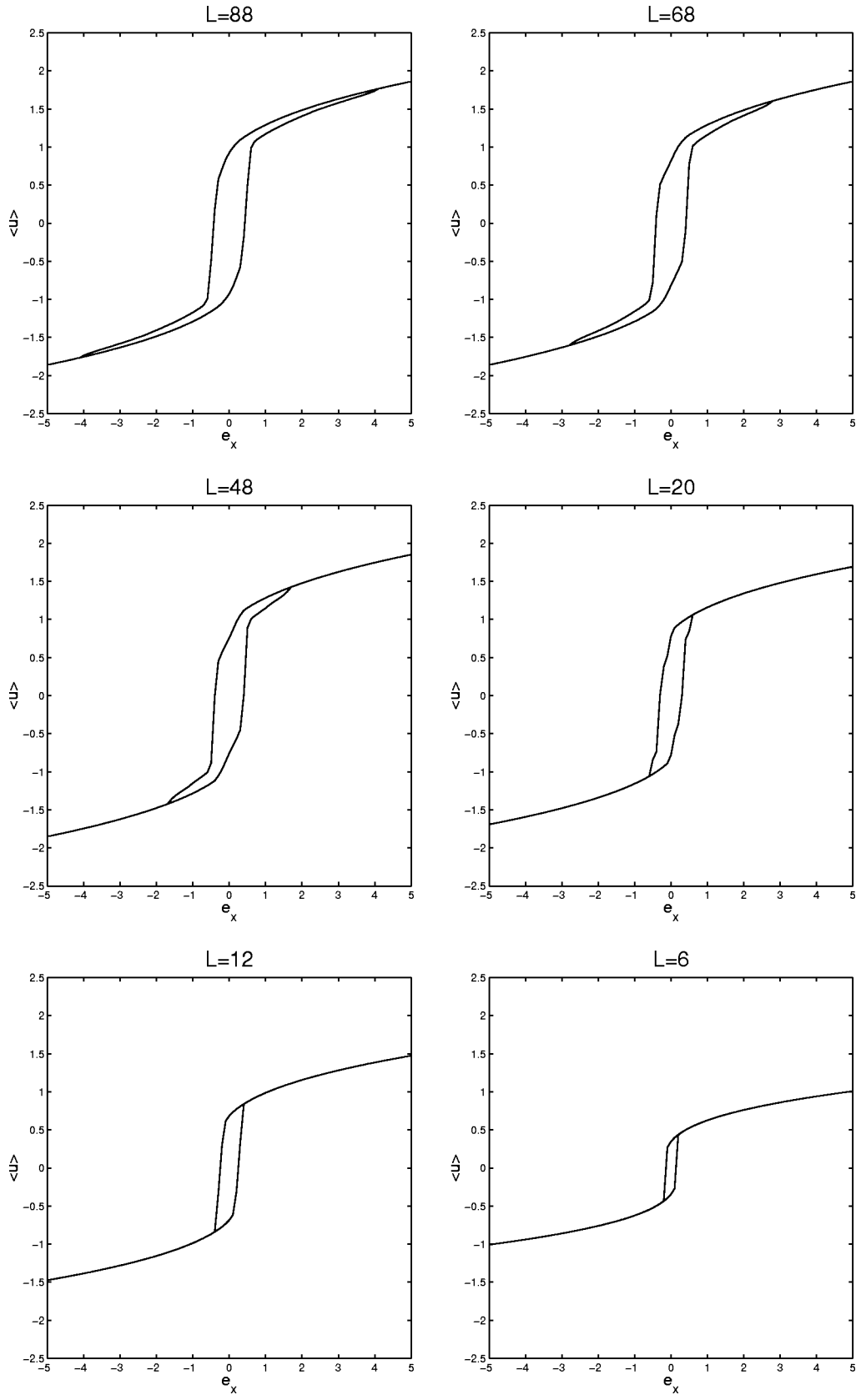

FIG. 3. Simulated hysteresis loops for different sizes of the constrained square.

of 90° domain walls. In contrast, for the semi-infinite geometry, there is no nucleation of 90° domains and the switching proceeds by 180° reversal. Clearly, the corners in the constrained square play a crucial role during the switching process. We believe that the anisotropy of the long-range elastic interaction interacts with the corners to produce inhomogeni-

Downloaded 25 Jun 2003 to 128.118.103.146. Redistribution subject to AIP license or copyright, see http://ojps.aip.org/japo/japcr.jsp

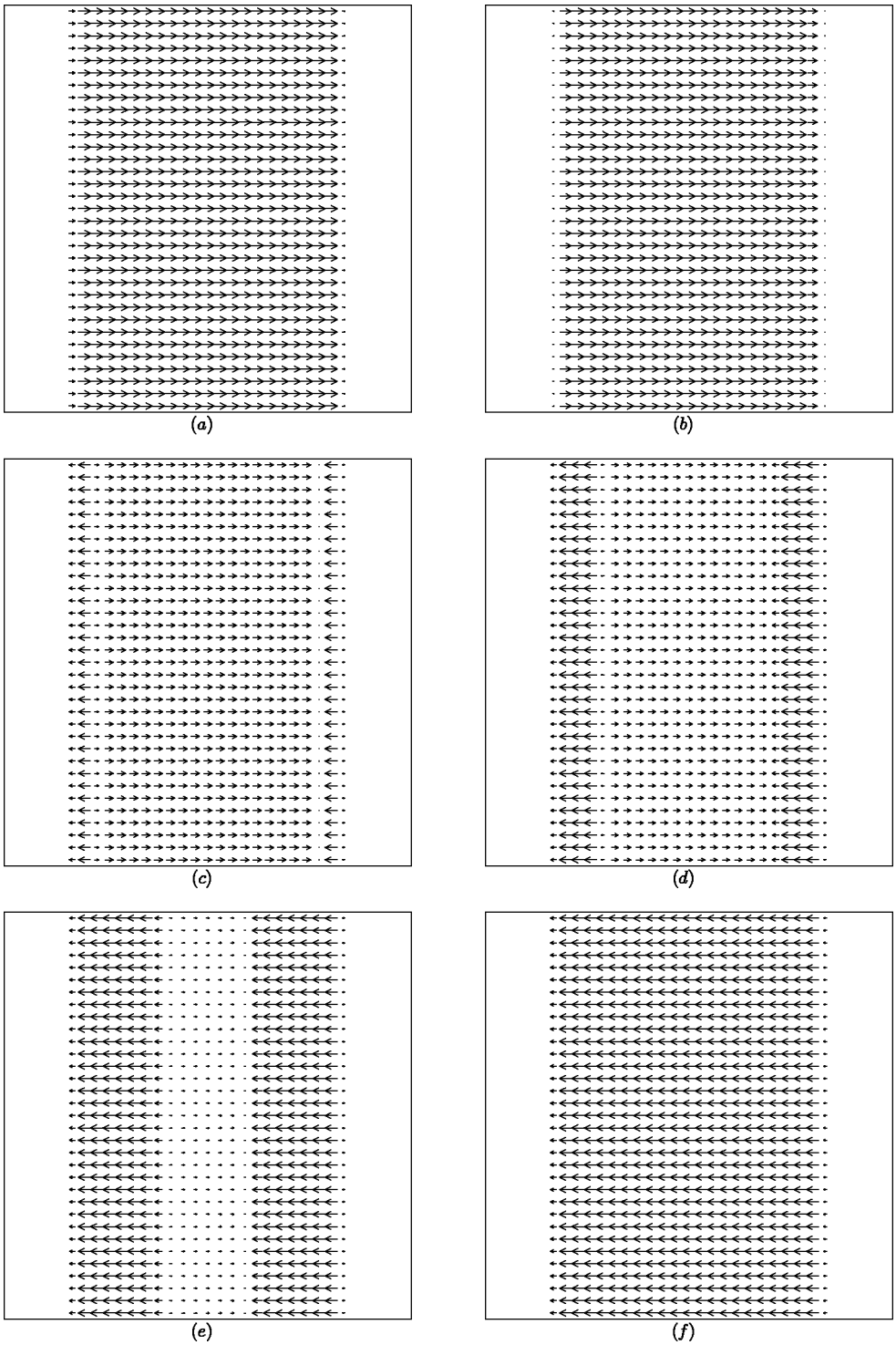

FIG. 4. Pattern evolution for the simulated switching in a semi-infinite constrained system. The snapshots correspond to (a) $e_{x*}=10$, (b) $e_{x*}=-0.319$, (c) $e_{x*}=-0.36$, (d) $e_{x*}=-0.399$, (e) $e_{x*}=-0.44$, and (f) $e_{x*}=-10$.

eties that result in 90° nucleation. Our results suggest that the switching behavior and the hysteresis loops in real systems may depend on the shape of the grain and its boundary conditions.

We have also simulated the size dependence of hysteresis loops. The decrease of the saturation polarization, remnant polarization, and the coercive field with decreasing size is common to both configurations. This can be understood in terms of the supression of the transition in an electromechanically constrained system as the system size approaches the correlation length of order parameter. The free energy for a constrained system is a function of the system size. For the constrained square case, the polarization reversal process is dominated by intermediate 90° domain pattern changes for larger systems and becomes totally via 180° reorientations for sizes less than a critical dimension. This transition is due to the weakening of the long-range elastic interactions with decreasing system size.

Downloaded 25 Jun 2003 to 128.118.103.146. Redistribution subject to AIP license or copyright, see http://ojps.aip.org/japo/japcr.jsp

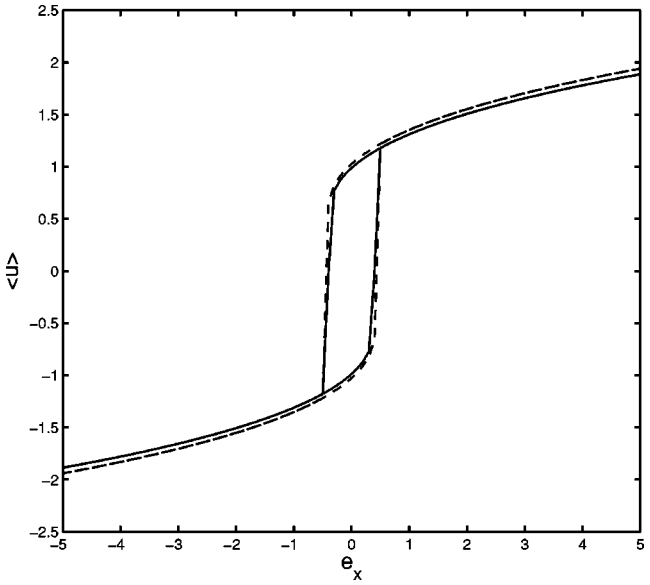

FIG. 5. Plots of $<u>$ vs e_x showing the simulated hysteresis loops for the semi-infinite constrained system (solid line) and the periodic boundary condition case (dotted line).

Finally, one should note that the behavior of decreasing coercive field with decreasing size indicated by the simulation results does not apply to thin films,[2] but only to clamped grains in ferroelectric polycrystals. For thin films, not all the dimensions are reduced simultaneously, which is different than our condition here. In addition, the misfit strain with the substrate is important, which has to be incorporated in the theory.[17]

ACKNOWLEDGMENT

This research was sponsored by the Hong Kong Research Grant Council under Grant No. CityU 1056/02P.

[1] M. E. Lines and A. M. Glass, Principles and Applications of Ferroelectrics and Related Materials (Clarendon, Oxford, 1979).
[2] S. Ducharme, V. M. Fridkin, A. V. Bune, S. P. Palto, L. M. Blinov, N. N. Petukhova, and S. G. Yudin, Phys. Rev. Lett. **84**, 175 (2000).
[3] R. Ahluwalia and W. Cao, Phys. Rev. B **63**, 012103 (2001).
[4] W. Y. Shih, W. H. Shih, and I. A. Aksay, Phys. Rev. B **50**, 15575 (1994).
[5] Y. G. Wang, W. L. Zhong, and P. L. Zhang, Phys. Rev. B **51**, 5311 (1995).
[6] E. Burscu, G. Ravichandran, and K. Bhattacharya, Appl. Phys. Lett. **77**, 1698 (2000).
[7] Wenwu Cao and L. E. Cross, Phys. Rev. B **44**, 5 (1991).
[8] E. A. H. Love, *A Treatise on the Mathematical Theory of Elasticity* (Dover, New York, 1944), p. 49.
[9] S. Kartha, J. A. Krumhansl, J. P. Sethna, and L. K. Wickham, Phys. Rev. B **52**, 803 (1995).
[10] S. R. Shenoy, T. Lookman, A. Saxena, and A. R. Bishop, Phys. Rev. B **60**, R12537 (1999).
[11] A. E. Jacobs, Phys. Rev. B **52**, 6327 (1995).
[12] A. E. Jacobs, Phys. Rev. B **61**, 6587 (2000).
[13] J. Yin and W. Cao, Appl. Phys. Lett. **79**, 4556 (2001).
[14] M. H. Frey and D. A. Payne, Phys. Rev. B **54**, 3158 (1996).
[15] R. Ahluwalia and W. Cao, J. Appl. Phys. **89**, 8105 (2001).
[16] G. Arlt, Ferroelectrics **104**, 217 (1990).
[17] N. A. Pertsev and V. G. Koukhar, Phys. Rev. Lett. **84**, 3722 (2000).

Downloaded 25 Jun 2003 to 128.118.103.146. Redistribution subject to AIP license or copyright, see http://ojps.aip.org/japo/japcr.jsp